Dissociable effects of visual crowding on the perception of color and motion

John A. Greenwood[a,1] and Michael J. Parsons[a]

[a]Department of Experimental Psychology, University College London, London WC1H 0AP, United Kingdom

Edited by Randolph Blake, Vanderbilt University, Nashville, TN, and approved February 20, 2020 (received for review June 12, 2019)

Our ability to recognize objects in peripheral vision is fundamentally limited by crowding, the deleterious effect of clutter that disrupts the recognition of features ranging from orientation and color to motion and depth. Previous research is equivocal on whether this reflects a singular process that disrupts all features simultaneously or multiple processes that affect each independently. We examined crowding for motion and color, two features that allow a strong test of feature independence. "Cowhide" stimuli were presented 15° in peripheral vision, either in isolation or surrounded by flankers to give crowding. Observers reported either the target direction (clockwise/counterclockwise from upward) or its hue (blue/purple). We first established that both features show systematic crowded errors (biased predominantly toward the flanker identities) and selectivity for target–flanker similarity (with reduced crowding for dissimilar target/flanker elements). The multiplicity of crowding was then tested with observers identifying both features. Here, a singular object-selective mechanism predicts that when crowding is weak for one feature and strong for the other that crowding should be all-or-none for both. In contrast, when crowding was weak for color and strong for motion, errors were reduced for color but remained for motion, and vice versa with weak motion and strong color crowding. This double dissociation reveals that crowding disrupts certain combinations of visual features in a feature-specific manner, ruling out a singular object-selective mechanism. Thus, the ability to recognize one aspect of a cluttered scene, like color, offers no guarantees for the correct recognition of other aspects, like motion.

perception | peripheral vision | crowding | color | motion

Our ability to recognize objects declines sharply in peripheral vision (1). This is not due simply to resolution or acuity: Objects that are visible in isolation become indistinguishable when other objects fall within surrounding "interference zones" (2–4). This process, known as crowding, presents a fundamental limit on peripheral vision, with pronounced elevations in central vision in disorders such as amblyopia (5) and dementia (6).

Crowded impairments arise due to a systematic change in the appearance of target objects (7, 8), particularly outside the fovea (9), where targets are induced to appear more similar to nearby "flankers." Crowding disrupts the recognition of features throughout the visual system, including orientation (10), position (11), color (12, 13), motion (14), and depth (15). Within these dimensions, crowding is also modulated by the similarity between target/flanker elements; differences in features, including orientation and color, reduce errors considerably (10, 16). Given the distributed processing of these features across the visual system (17, 18), can one process produce this multitude of effects? Most models implicitly assume that crowding is a single mechanism that affects all features in a combined manner, particularly for higher-order approaches where crowding derives from attention (19, 20) or grouping (21). If crowding were instead to operate independently for distinct visual features, these effects could involve an array of neural substrates with varied mechanisms.

A key prediction for a combined crowding process is that a release from crowding in one feature domain (e.g., color) should release other features (e.g., motion) at the same time. Accordingly, target–flanker differences in color or contrast polarity can reduce crowding for judgments of spatial form (16), while differences in orientation improve crowded position judgments (22). However, others have found that judgments of spatial frequency, color, and orientation show a mixture of independent and combined errors (23). This discrepancy may reflect the specific features used in each study. Here we examined whether crowding is combined or independent for judgments of motion and color—arguably the two features with the clearest separation in the visual system (17, 18).

We conducted three experiments with motion and color, each using cowhide-like stimuli (24, 25) in the upper visual field. Experiments 1 and 2 examined crowding for each feature separately to determine both the nature of the errors (i.e., their systematicity) and the flanker conditions that give strong vs. weak crowding. We then measured the independence of crowding with conjoint motion/color judgments in Experiment 3 by selecting conditions in which crowding was strong for one feature and weak for the other, or vice versa.

Results

In Experiment 1, observers viewed moving cowhide stimuli and reported the movement direction (clockwise [CW] or counterclockwise [CCW] of upward) of a target presented either in isolation or surrounded by flankers moving in one of 16 directions (Fig. 1*A* and Movie S1). Example data are shown in Fig. 1*B*, where unflanked

Significance

Our peripheral vision is primarily limited by crowding, the disruption to object recognition that arises in clutter. Crowding is widely assumed to be a singular process, affecting all the features (e.g., orientation, motion, color) within an object simultaneously. In contrast, we observe a double dissociation whereby observers make errors regarding the color of a crowded object while correctly judging its direction, and vice versa. This dissociation can be reproduced by a population-coding model in which the direction and hue of target/flanker elements are pooled independently. The selective disruption of some object features independently of others rules out a singular crowding mechanism, posing problems for high-level crowding theories and suggesting that the underlying mechanisms may be distributed throughout the visual system.

Author contributions: J.A.G. and M.J.P. designed research; J.A.G. and M.J.P. performed research; J.A.G. and M.J.P. analyzed data; J.A.G. developed models; and J.A.G. wrote the paper.

The authors declare no competing interest.

This article is a PNAS Direct Submission.

Data deposition: MATLAB code for psychometric functions and stimulus generation is available at https://github.com/eccentricvision.

[1]To whom correspondence may be addressed. Email: john.greenwood@ucl.ac.uk.

This article contains supporting information online at https://www.pnas.org/lookup/suppl/doi:10.1073/pnas.1909011117/-/DCSupplemental.

First published March 19, 2020.

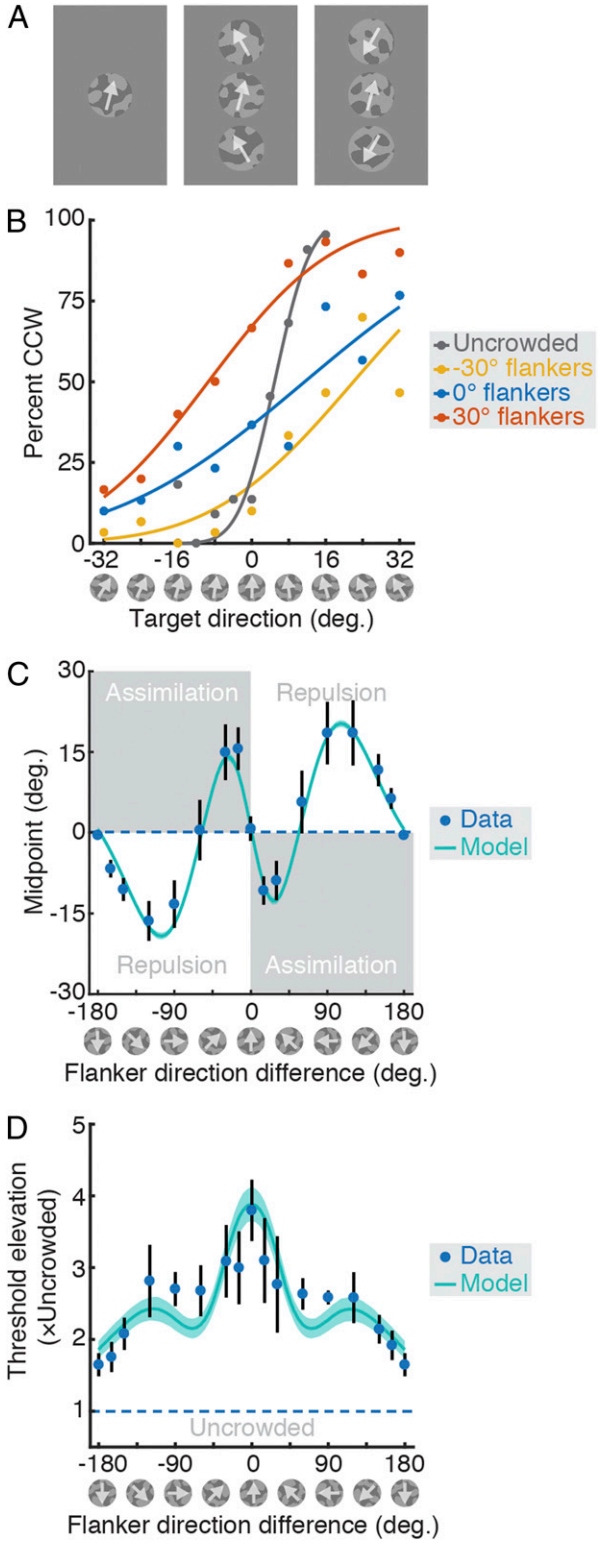

Fig. 1. The effect of crowding on motion perception (Experiment 1). (*A*, *Left*) An unflanked cowhide stimulus. (*A*, *Middle*) A crowded array with the target between flankers moving 30° CCW of upward. (*A*, *Right*) Crowded by flankers moving 150° CCW of upward. (*B*) Example data and psychometric functions for observer YL, with the proportion of CCW responses plotted as a function of target direction. Data are shown for an unflanked target (gray) and with flankers moving upward (blue), −30° CW of upward (yellow), and 30° CCW (red). (*C*) Midpoint (PSE) values averaged over six observers (blue points with error bars ±1 SEM), plotted as a function of flanker direction. The mean output of a population crowding model is shown (green line) surrounded by the 95% range of values. (*D*) Threshold elevation values for the same conditions, plotted as in *C*.

judgments (gray points) transition rapidly from predominantly CW to CCW at directions around upward (0°). The psychometric function accordingly shows low bias in the Point of Subjective Equality with upward (PSE; the 50% midpoint), with the steep slope indicating a low threshold (the difference from 50% to 75% CCW responses). With upward-moving flankers (+0°; blue points) performance declined, with a shallower psychometric function, but nonetheless remained unbiased. In contrast, flankers moving 30° CCW of upward (red) induced a strong bias toward CCW responses, causing a leftward shift of the function in addition to the shallower slope. The opposite bias arose with CW flankers (yellow). Thus, both aspects of crowding are captured here: assimilative errors via the PSE and the impairment in performance via threshold values.

Psychometric functions were fit separately for each flanker condition and observer. Mean PSE values across observers are plotted as a function of the target–flanker difference in Fig. 1*C*. On average, upward-moving flankers (0°) did not induce any bias, as with the example observer. Flankers moving slightly CW (e.g., −15°) induced a positive PSE shift, indicating an increase in CW responses. These assimilative errors were mirrored for small target–flanker differences in the CCW direction. Larger target–flanker differences (e.g., ±90°) induced a repulsive PSE shift, indicating that the perceived target direction was biased away from that of the flankers. Further increases gave a reduction in bias, with downward flankers inducing no bias on average. Threshold elevation values (flanked thresholds divided by unflanked thresholds) are shown in Fig. 1*D*, where a value of 1 indicates performance equivalent to unflanked thresholds (dashed line). The greatest threshold elevation occurred with upward-moving flankers, with a decline in threshold elevation as flanker directions diverged. Downward-moving flankers gave the least threshold elevation, although values remained >1 for all observers. Altogether, crowding was strong with assimilative errors when target–flanker differences in motion were small and reduced for large target–flanker differences with either repulsive errors or minimal biases.

We next examined the effect of crowding on judgments of hue in Experiment 2. Here observers identified whether the target was blue/turquoise or purple/pink (Fig. 2*A* and Movie S2). When present, flankers differed from the reference hue by one of 12 hue angles in the Derrington–Krauskopf–Lennie (DKL) color space (26–28). Example data are shown in Fig. 2*B*. Flankers with the same hue as the reference boundary (0°; blue points) did not induce any bias, although the slope was shallower than when unflanked (gray points). Flankers with a purple +15° hue angle (purple points) induced both a shallower slope in the psychometric function and a shift in the PSE, indicating assimilative errors, as did the blue −15° flankers (turquoise points).

Fig. 2*C* plots the mean PSE values for all flanker conditions. As with motion, flanker hues at the decision boundary (0°) induced no bias on average. Flankers with CW hue differences (blue to green in appearance) also induced positive shifts in PSE, indicating an increase in blue responses. Assimilative errors were again mirrored for flankers with CCW hue angles, ranging from purple/pink to red, while larger target–flanker differences showed little to no assimilative bias. Unlike motion, no errors of repulsion were observed. Mean threshold elevation values are shown in Fig. 2*D*. Although threshold elevation values are lower than those for motion, the patterns of data are broadly similar, with the greatest threshold elevation for small target–flanker differences and a decrease in crowding strength with increasing difference. Flankers with the greatest differences (yellow/brown hues) did not elevate thresholds relative to unflanked performance.

Overall, the crowding of both motion and color is selective for target–flanker similarity; threshold elevation is high with small

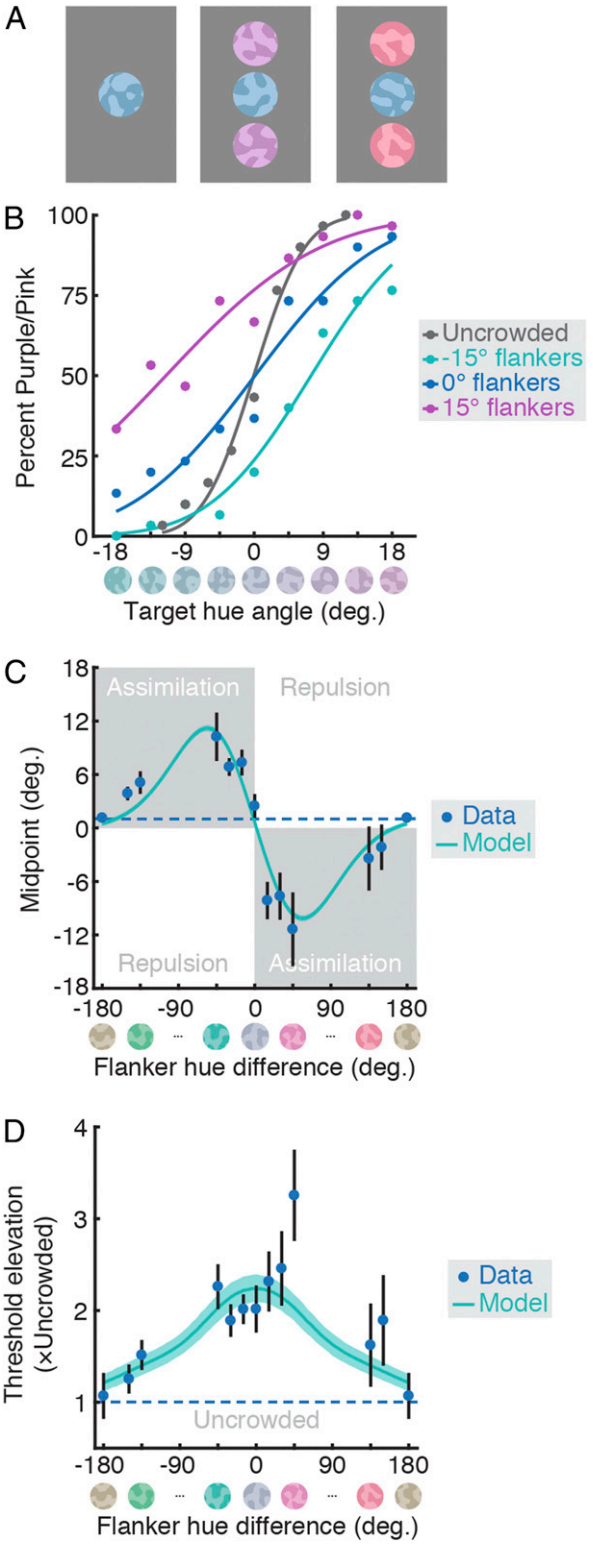

Fig. 2. Crowding for color perception (Experiment 2). (*A*, *Left*) An unflanked stimulus. (*A*, *Middle*) A flanked array with the target between flankers with +15° hues (purple). (*A*, *Right*) A target with +135° flankers (pink/red). (*B*) Example data and psychometric functions for observer AK, plotting the proportion of trials with a purple/pink response as a function of target hue (depicted on the *x*-axis). Data are shown for an unflanked target (gray) and flanked by stimuli with hues near the decision boundary (blue points), +15° CCW (purple), and −15° CW (turquoise). (*C*) Midpoint (PSE) values averaged over six observers (blue points ±1 SEM), plotted as a function of flanker hue. The mean output of a population model of crowding is shown (green line), surrounded by the 95% range of values. (*D*) Threshold elevation values for the same conditions, plotted as in *C*.

target–flanker differences and low with larger differences. In both cases, crowding also produced systematic errors that were predominantly assimilative for small target–flanker differences and declined with larger differences (although direction errors were repulsed at intermediate differences, which was not apparent for hue). More generally, the results of both experiments are broadly consistent with observations that biases follow the derivative of squared thresholds in a range of perceptual domains (29).

With this knowledge, we can now make predictions for paired judgments of motion and color. Namely, when crowding is strong for one feature (with small target–flanker differences, e.g., in direction) and weak for the other feature (with larger differences, e.g., in hue), independent crowding processes allow assimilative errors to occur for the feature with strong crowding without errors for the feature with weak crowding. In contrast, a combined mechanism predicts that crowding must be all or none: If crowding is weak for one feature, then it must be either reduced or persist for both.

Experiment 3 was designed to distinguish between these alternatives. Observers made conjoint judgments of the direction (CW/CCW of upward) and hue (blue/pink) of the target cowhide for isolated targets and in three crowding strength conditions. In the first of these conditions, crowding was strong for both features, with small target–flanker differences in direction and hue (Movie S3). In the second condition (Movie S4), crowding was weak for direction (large direction difference) and strong for hue (small hue difference). The third condition (Movie S5) involved strong crowding for direction (small differences) and weak crowding for hue (large differences). Each crowding strength condition had four combinations of motion and color for target and flanker elements with respect to the decision boundary in each feature dimension: both match (e.g., CW moving target and flankers, all blue in hue), motion differs (e.g., a CW target with CCW flankers, all purple), color differs (e.g., a purple target with blue flankers, all moving CW), or both differ. The crucial condition is when both differ; here, the all-or-none combined mechanism predicts errors either in both features or in neither feature, while the independent mechanism allows a reduction in crowding in one feature without affecting the other feature.

With an unflanked target, observers correctly identified its direction in 87.71 ± 3.29% (mean ± SEM) of trials and its hue in 93.96 ± 1.76% of trials. Fig. 3*A* shows mean responses for the first crowding strength condition, with strong crowding for both features. When target and flankers were matched in both feature dimensions (red point), performance was high in both cases. Here, even if crowding occurred, the assimilative effect of the flankers would pull responses toward the correct direction/hue. In the motion differs condition, observers were largely correct on the hue and incorrect for direction. This again is predicted by assimilative errors for direction, with either no effect on hue or assimilative crowding toward the correct hue. The converse occurred for the color differs condition, with a predominance of color errors. Finally, in the both differ condition, the strong assimilation for direction and hue induced errors for both features.

Fig. 3*B* shows results from the weak motion + strong color crowding condition. As before, in the both match condition, responses were correct on both features. In the motion differs condition, the large direction difference gave a reduction in crowding, with predominantly correct responses for direction and likewise for hue given the matched target and flanker colors. For the color differs condition, the small hue difference continued to induce assimilative errors, while the similar target and flanker directions gave either assimilative errors or correct target

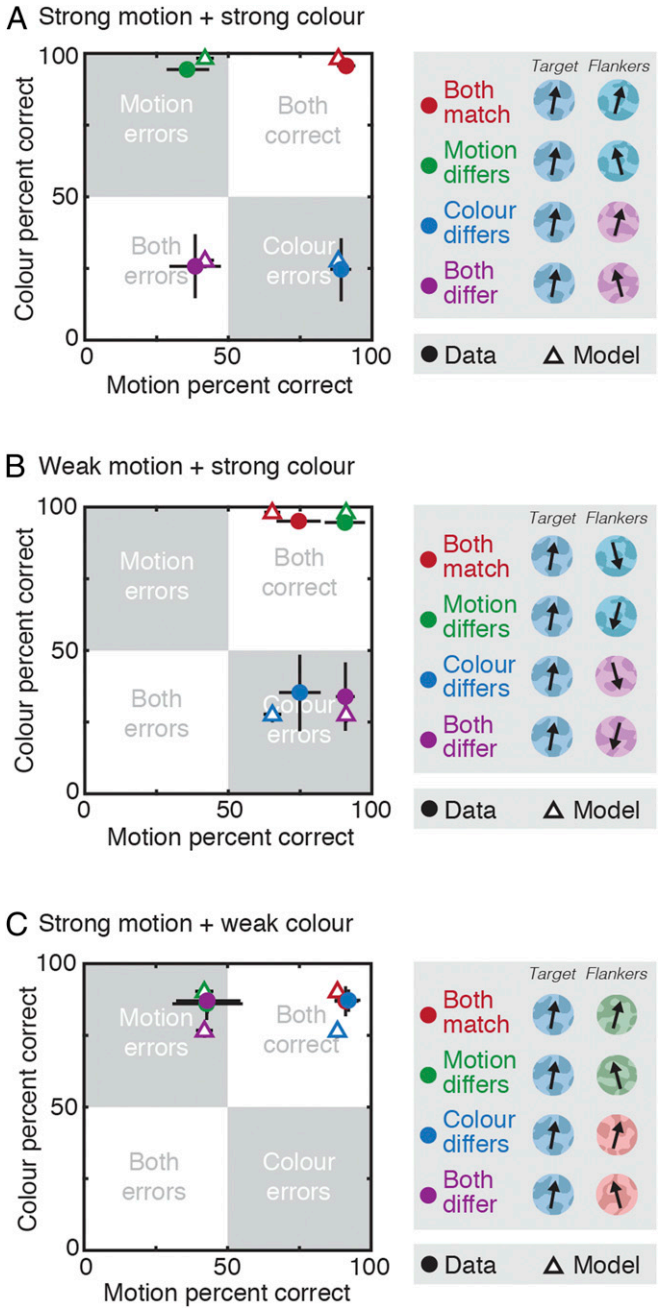

Fig. 3. Results from the conjoint crowding of motion and color (Experiment 3). Data (circles) are plotted as the mean ±1 SEM proportion correct (n = 6) for the target direction (x-axis) and hue (y-axis). The mean ±1 SEM output of the best-fitting independent crowding model (triangles) with separate weights for motion and color is also shown. Quadrants are demarcated to show the predominant error type (e.g., "motion errors"). In each crowding strength condition (separate panels), there were four target–flanker match conditions (depicted in the legend) in which the 2AFC sign was matched for both features, the motion differed, the color differed, or both differed. (*A*) Strong motion + strong color crowding. (*B*) Weak motion + strong color crowding. (*C*) Strong motion + weak color crowding.

recognition. Crucially, in the both differ condition, responses were correct for direction (as in the motion differs condition) but errors remained for hue, shifting responses into the "color errors" quadrant. Overall, the reduction in motion errors causes data for all conditions to align along the x-axis, while the separation along the y-axis for color is retained. In other words, crowding was weak for motion and strong for color in the same stimulus.

The converse pattern can be seen in the strong motion + weak color condition (Fig. 3*C*). Responses were again close to ceiling in the both match condition. In the motion differs condition, the small target–flanker direction difference again induced a high rate of assimilative motion errors and a low rate of color errors. Here in the color differs condition, the large color difference reduced crowding for hue judgments, while the matched target and flanker signs for direction led to correct responses for both features. Finally, the both differ condition again revealed a dissociation: Large differences in target–flanker hue coupled with a small difference in direction produced errors in direction responses despite correct responses for hue. Thus, the reduction in color crowding collapses data along the y-axis, while the separation for motion errors on the x-axis is retained. Here too, crowded errors can occur for one feature and not for the other feature.

These errors follow the prediction of independent crowding processes for motion and color and are inconsistent with the predictions of a combined mechanism, whereby errors should have clustered in either the "both correct" or the "both errors" quadrant. Accordingly, although errors in the both differ condition appear to be correlated on a trial-by-trial basis when crowding is strong for both features (*SI Appendix*, Fig. S1*A*), this correlation breaks down when crowding is reduced for either feature (*SI Appendix*, Fig. S1 *B* and *C*). We have further replicated these results with an increase in crowding strength; with additional flankers, we find stronger modulation in the crowding of motion and color (*SI Appendix*, Fig. S2), but the pattern of independent errors for conjoint judgments of the two features remains (*SI Appendix*, Fig. S3). Finally, we also report that these dissociations in crowding are not confined to motion and color; conjoint judgments of luminance contrast polarity and direction show that errors can be low for contrast polarity and yet remain high for the direction of the same stimulus (*SI Appendix*, Fig. S4).

Models. To better understand the mechanisms underlying these errors, and for the quantitative comparison of combined vs. independent mechanisms, we developed a set of computational models. Given the systematicity of crowded errors in these experiments, the most plausible models are those based on averaging or substitution (7, 11). A more general approach has been shown to produce both averaging and substitution errors by combining population responses to target/flanker elements (30). Thus, to simulate motion crowding in Experiment 1, we developed a model population of direction detectors, with responses to target and flanker directions combined according to a weighting field. Whereas previous studies have used weighting fields that decreased with target–flanker distance (30), here the weights altered crowding strength as a function of target–flanker dissimilarity. To simulate the observed repulsion errors, we incorporated inhibitory interactions between target and flanker population responses, similar to models of the tilt illusion (31, 32). Further details and best-fitting parameters are provided in the *SI Appendix*.

The best-fitting simulations of the crowded biases for motion in Experiment 1 are shown in Fig. 1*C* (green line). The model follows the increase in assimilative bias with small target–flanker direction differences, driven by summation of the target and flanker population responses. It also captures the rise and fall of repulsion with larger differences, driven by inhibition of the target (*SI Appendix*, Fig. S5). Similarly, threshold elevation values (Fig. 1*D*) show the greatest elevation for small direction differences, with a decline on either side.

A similar population model was developed for color crowding in Experiment 2 (*SI Appendix*, Fig. S5). Given the lack of repulsion for color, inhibitory model parameters were set to 0. Fig. 2*C* plots simulated biases (green line), which again capture the strong assimilative errors with small target–flanker hue

differences and the decrease in these errors at larger differences. Threshold elevation values are similarly well described (Fig. 2*D*), with a strong impairment for small target–flanker differences that progressively declines. Thus, population coding models can capture the errors observed for color as well as for motion.

We next used these population models to simulate the conjoint motion and color judgments of Experiment 3. Given the independent pattern of errors observed, here we focus on the operation of an independent crowding model in which responses to target and flanker elements were combined via separate weighting fields for direction and hue (see *SI Appendix* for full details). The independence of these weights meant that the strength of crowding for one feature did not affect the other feature. Fig. 3*A* shows the best-fitting simulations for this model in the strong motion + strong color condition, which closely follow the pattern of data because the probability of crowding is high for both features. The model performs similarly well in the weak motion + strong color condition (Fig. 3*B*) because the separate weights allow crowding to be decreased for motion but not for color, leaving a predominance of color errors in the both differ condition. Similarly, in the both differ condition with strong motion + weak color crowding (Fig. 3*C*), errors were decreased for color but remained strong for motion. Overall, the model closely follows the observed pattern of errors.

We also developed a range of "combined" models that use the same weight to crowd motion and color on each trial. As outlined in the *SI Appendix*, these models consistently fail to replicate the pattern of errors found in Experiment 3 (*SI Appendix*, Figs. S6 and S7). Variations of the combined mechanism do little to improve performance; models that use the minimum or maximum probability for crowding in both features and those with a single weighting field all produce worse fits than the independent model. Regardless of the precise mechanism, the crowding of motion and color is best explained by independent processes.

Discussion

Our perception of motion and color is disrupted by crowding. Here we show that these effects are dissociable, indicating that they derive from independent processes. In Experiment 3, observers made judgments of both features while we manipulated the strength of crowding separately for each, using values from Experiments 1 and 2. When crowding was weak for motion (via large target–flanker direction differences) and strong for color (via small differences), errors were reduced for motion but remained high for color. Similarly, a reduction in color crowding did not reduce errors for judgments of the target direction. A population coding model of crowding reproduced this double dissociation by pooling target and flanker signals with independent weights for motion and color. Models in which crowding operated as a combined all-or-none process (with matched crowding strength for both features) failed to replicate these results.

Dissociations were also evident in the crowded errors for motion and color measured in Experiments 1 and 2. First, the overall magnitude of biases and threshold elevation was lower for color than for motion. This difference diminished with additional flankers (*SI Appendix*, Fig. S2), further suggesting that crowding increases with flanker number at different rates for the two features. Second, intermediate target–flanker differences in motion caused a repulsion in perceived target direction, while equivalent color differences simply reduced the rate of assimilative errors. Our population models reproduced these patterns via inhibitory interactions for motion, which were absent for color. Of course, this does not mean that contextual modulations for color are never repulsive. Although similar contextual effects tend toward assimilation in the periphery (33), repulsion in the perceived hue of targets does occur in foveal vision (34). A progression from foveal repulsion to peripheral assimilation also occurs for orientation (9). Given that motion repulsion occurs in both foveal and peripheral vision (35), it may be that the progression from repulsion to assimilation is more rapid across eccentricity for color than for motion. In other words, these distinct patterns of crowded errors offer further support for independent processes, although they may reflect variations in a common principle.

Although these dissociations for motion and color crowding are consistent with the separation between these features in the visual system (17, 18), our findings differ from those of previous studies using other feature pairs. We attribute this difference to the degree of separation between these features in the visual system. For instance, the mixed pattern of independent and combined errors with spatial frequency, color, and orientation (23) may have arisen because color is dissociable from orientation and spatial frequency, as has been suggested recently (36), while orientation and spatial frequency are more closely linked. Similarly, the combined pattern of errors found for orientation and position crowding (22) could reflect the interdependence of these features (37). That is, features that are closely related in the visual system may show linked performance, while more distinct feature pairs give dissociable effects. Comparable patterns are evident in other visual processes; for instance, color and orientation show independent decay rates in visual working memory, unlike more closely linked spatial dimensions (38). A strong feature association could similarly explain the release in crowding for spatial form judgments by differences in color or contrast polarity (16). However, in these cases, the spatial forms are typically defined by the differential features (i.e., the spatial distribution of color/polarity gives both the object surface and its boundaries; ref. 39), making the color or polarity signals informative regarding the feature being judged. Dissociations may become evident only when features can be judged independently, as in the present study.

Importantly, however, a single dissociation between features is sufficient to reject an object-selective mechanism. Our results rule out this mechanism with at least two dissociations: color and motion (Fig. 3) and contrast polarity and motion (*SI Appendix*, Fig. S4). These results are similarly inconsistent with higher-level theories of crowding. Gestalt approaches (21) argue that crowding occurs when the target is "grouped" with the flankers—for example, by forming a pattern with the flankers (40)—and that it is reduced when the flankers form patterns that exclude the target (41). The top-down nature of grouping suggests that it should apply to the collection of features within the target as a whole, making it an all-or-none process that is inconsistent with the dissociations found here. Our findings are equally unlikely to be accounted for by attentional theories (19, 20), since the high-level nature of attentional selection predicts that crowding should operate at the level of objects or locations rather than being divisible for specific features within a localized target. Of course, attention and grouping could certainly modulate the strength of crowding—our findings simply suggest that these processes are not central to crowding.

Our population-coding model of these effects is similar to previous approaches in crowding and related contextual modulations (30–32). Here we show their generalizability to the domains of motion and color. In fact, the dissociable nature of crowding lends itself to this approach; distinct populations with independent weighting fields for these features require fewer assumptions than a combined mechanism (*SI Appendix*, Fig. S6). Population coding may also explain the aforementioned distinction between combined crowding errors with some feature pairs and independent errors with others; the separation between these features in a multidimensional space, driven perhaps by their cortical distance (9, 42) could determine the nature of these target–flanker interactions. Of course, it is also possible that "texturization" models (43–45) could reproduce many of these effects, although distinct spatial and temporal texture

processes would be needed to reproduce the dissociations for motion and color.

The dissociation between motion and color crowding further suggests that they may rely on distinct neural substrates. The many neural correlates of crowding reported from V1 through V4 (46–49) may in fact reflect this distributed nature. In the most minimal sense, crowding in the ventral stream (44) may differ from the dorsal stream processes (17) likely involved in the crowding of motion. Crowding effects for other dissociable feature pairs may then be distributed similarly. It follows that crowding may be more profitably viewed as a general property of the visual system, similar to distributed processes like adaptation that affect a range of visual features (50). However, it is also possible that dissociations could arise within a single cortical region through the operation of distinct neural subpopulations, as has been argued for feature-binding processes (51).

At first glance, the distributed basis of these crowding effects bears some similarity to multilevel theories of crowding (4). However, these theories are based on an apparent uniqueness in the crowding of faces (52, 53), an effect that disappears once task difficulty is equated for upright and inverted faces (54). Although we did observe some differences in the crowding of motion and color (e.g., with repulsion for motion vs. pure assimilation for color), the broad selectivity of crowding was nonetheless highly similar in Experiments 1 and 2. Namely, small target–flanker differences gave strong assimilative errors and high threshold elevation for both features, while large differences gave a reduction in threshold elevation. In other words, wherever crowding occurs, it follows similar principles.

One complication with this distributed view of crowding is the common size of interference zones observed across a range of visual features (Bouma's law; refs. 2, 3, and 12). Although differences may yet emerge for the specific comparison of motion and color, this common spatial region may again be consistent with our effects deriving from distinct neural subpopulations with varying featural selectivity but common spatial properties. Alternatively, the proximity of target and flanker signals on the cortical surface (9, 42) may determine their potential for interaction, while the specific features present determine the nature of these interactions.

Taken together, our findings demonstrate that crowding independently disrupts motion and color while nonetheless operating via common principles, as seen in the implementation of our population models. This dissociation excludes the possibility that crowding operates as a singular mechanism and suggests that at least some aspects of vision are disrupted by clutter in a feature-specific manner.

Materials and Methods

Observers. Six observers (three males, including the authors) completed all three experiments. All had normal or corrected-to-normal acuity and normal color vision as assessed by the Ishihara test (55). Informed consent was given, with procedures approved by the Experimental Psychology Ethics Committee at University College London.

Apparatus. Experiments were programmed in MATLAB (MathWorks) on an Apple Mac Pro using the PsychToolbox (56, 57). Stimuli were presented on a 21″ Mitsubishi Diamond Plus CRT monitor with a resolution of 1,400 × 1,050 pixels and a 75-Hz refresh rate. The monitor was calibrated using a Minolta photometer and linearized in software to give a mean luminance of 50 cd/m^2, a maximum luminance of 100 cd/m^2, and a white point near the standard CIE Standard Illuminant D65. Maximum luminance values for red, green, and blue were 28.3, 69.5, and 8.1 cd/m^2, respectively. Observers viewed stimuli binocularly from a distance of 50 cm, with head movements minimized using a head and chin rest. Responses were given via a keypad, with auditory feedback provided only during practice sessions.

Stimuli and Procedures. In all experiments, target and flanker stimuli were cowhide elements (24, 25), created by bandpass filtering white noise with a spatial frequency cutoff of 1.5 cycles/degree and rounding the luminance to give two values (light and dark). Each element was presented within a circular aperture with 2° diameter. The visible contours in these elements enabled the perception of motion with minimal ambiguity given their orientation variance (i.e., avoiding the aperture problem; ref. 24), while also allowing alteration of the surface hue.

Observers were required to maintain fixation on a two-dimensional Gaussian blob with an SD of 4′. The target was presented 15° above fixation, either in isolation or with one flanker above and one below. The center-to-center separation of target and flankers was 2.25°, corresponding to 0.15 times the eccentricity (well within standard interference zones; refs. 2 and 3). Stimuli were presented for 500 ms, followed by a mask for 250 ms (a patch of 1/f noise in a circular window of diameter 4.8° when unflanked and 8.5° when flanked, plus a cosine edge). The mask was followed by a mean-gray screen with the fixation point, at which time observers responded.

In Experiment 1, cowhide stimuli were gray-scale elements with a Weber contrast of ±0.75 against the mean-gray background. Patches were generated as a long strip of texture that moved behind the aperture with a displacement of 5.8′ per frame every second monitor frame (to allow greater resolution of directional displacements with larger, less frequent steps). This gave an effective stimulus refresh rate of 37.5 Hz and a speed of 3.6 deg/s.

When unflanked, the target moved in one of nine equally spaced directions between ±16° around upward and ±32° when flanked (given the greater difficulty). Observers indicated whether the target moved CCW or CW of upward. When present, flankers moved together in one of 16 directions relative to upward: 0°, ±15°, ±30°, ±60°, ±90°, ±120°, ±150°, ±165°, or 180°. Each block had 10 repeat trials per target direction, giving 90 trials for unflanked blocks and 180 trials for flanked conditions, in which opposing flanker directions (e.g., ±15°) were interleaved within a single block to ensure a balanced likelihood of CW and CCW responses. The 0° and 180° conditions were also interleaved for consistency. Each block was repeated three times, with all blocks randomly interleaved, to give 4,590 total trials per observer, plus practice, completed in three or four sessions of 1 h each.

In Experiment 2, cowhides were static and presented with a range of hues. Colors were determined using the DKL color space (26–28) with a luminance contrast of ±0.3 for light and dark regions and a color contrast/saturation of 0.2. Variations were applied solely to the hue angle. The reference hue angle was determined individually, given variation in the categorical boundaries for color between observers (28). We did so by presenting the test range of hues (from blue/turquoise to pink/purple) and asking observers to indicate the neutral midpoint. This gave a reference hue of 262.5° for four observers, 262.0° for JG, and 264.0° for CS. When unflanked, the target was presented with one of nine equally spaced hues ±12° from the base hue, and from ±18° when flanked. Observers judged whether the target appeared blue/turquoise (CW in DKL space) or purple/pink (CCW). When present, flankers had one of 12 hue angles relative to the base: 0°, ±15°, ±30°, ±45°, ±135°, ±150°, and 180°, tested in blocks that contained opposing angles as above. This gave 90 trials per unflanked block and 180 trials when flanked, giving 3,510 total trials per observer, plus practice, completed in three sessions.

In Experiment 3, cowhides varied in both direction and hue. For each observer, we selected values from the first two experiments that gave near-ceiling performance levels when unflanked but that were clearly impaired by crowding in the strongest crowding conditions. This gave values of ±5° (YL), ±6° (CS and JG), ±7° (DO), ±10° (AK), and ±16° (MP) for direction and ±3° (CS and YL), ±4° (DO), ±5° (JG), ±7° (AK), and ±10° (MP) for hue. Observers indicated the direction and hue of the target as a 4AFC response: blue/CCW, blue/CW, pink/CCW, or pink/CW. Targets were presented either in isolation or with flankers selected for each feature to give either "strong" or "weak" crowding (as above). Strong flanker directions were ±10° (DO), ±15° (AK, CS, JG, and YL), and ±30° (MP), with weak values of ±165° (five observers) and ±175° (AK). Strong flanker hues were ±15° (AK and YL) and ±30° (the remainder), with weak values of ±150° (five observers) and ±165° (JG).

In addition to the unflanked condition, the above combinations of target and flanker elements gave three crowding strength conditions: strong motion + strong color crowding (small target–flanker differences for each), weak motion + strong color crowding (large motion, small color differences), and strong motion + weak color crowding (small motion, large color differences). For flanked conditions, there were 16 combinations of direction and hue values in the target and flanker elements (2 target directions × 2 flanker directions × 2 target hues × 2 flanker hues). We grouped these conditions into four combinations of target/flanker elements in terms of their agreement in the 2AFC decision space for each feature. In the both match conditions, both motion and color were matched in target and flanker elements. When motion differed, the sign of the target direction differed from that of the flankers (e.g., a CW target with CCW flankers), but their hues matched. Conversely, when color differed, the hue of the target differed from the flankers, while directions were matched. Finally, both target and flanker elements could differ in direction and hue values. Note that these distinctions relate to the decision boundary,

ignoring precise values of direction/hue (e.g., –15° and –165° flankers have the same sign as a –8° target). The four crowding strength conditions were tested in separate blocks, with each combination of target and flanker elements repeated 10 times per block to give 40 trials when unflanked and 160 trials for flanked conditions. Each block was repeated six times, interleaved at random, with 3,120 total trials per observer (plus practice), completed in three sessions.

Analyses. In Experiments 1 and 2, psychometric functions were fit to data as a cumulative Gaussian function with three free parameters: midpoint/PSE (at 50%), slope, and lapse rate. Functions were fit separately for each flanker condition and observer. Shifts in the midpoint were taken as changes in appearance (i.e., assimilation vs. repulsion errors). Thresholds were taken as the difference in direction/hue required to shift performance from the midpoint to 75% CCW responses, with threshold elevation obtained by dividing flanked thresholds by unflanked thresholds. Data in Experiment 3 were combined from the 16 target–flanker combinations into four target–flanker match conditions and analyzed as the percent correct in each feature dimension, with each treated as a 2AFC judgment.

Models. Data in Experiments 1 and 2 were fit with a population coding model based on that of Harrison and Bex (30). The motion crowding model of Experiment 1 had nine free parameters, with five free parameters for the color model in Experiment 2 (since the lack of repulsion allowed inhibitory components to be removed), as described in the *SI Appendix* and depicted in *SI Appendix*, Fig. S5. *SI Appendix*, Table S1 shows the best-fitting parameters, with final outputs in Figs. 1 and 2. In Experiment 3, the independent model for motion and color crowding involved population responses to target and flanker elements that were combined via separate weighting fields for each feature. The majority of parameters were carried forward from Experiments 1 and 2, leaving three free parameters (*SI Appendix*, Table S2). Outputs of the best-fitting model are shown in Fig. 3. A series of combined models were also developed that were identical to the independent model except for the use of common weights for both features. *SI Appendix*, Tables S3 and S4 present the best-fitting parameters, and outputs are shown in *SI Appendix*, Figs. S6 and S7. Parts of this work were previously presented to the Vision Sciences Society (58).

Data Availability Statement. Datasets S1–S3 provide data in proportion of CCW format for each observer in Experiments 1 and 2 and in proportion of correct format for each observer in Experiment 3. MATLAB code for psychometric functions and stimulus generation is available at https://github.com/eccentricvision.

ACKNOWLEDGMENTS. Thanks to Alexandra Kalpadakis-Smith, Samuel Solomon, and Christoph Witzel for helpful comments. This work was funded by a UK Medical Research Council Career Development Award (MR/K024817/1).

1. R. Rosenholtz, Capabilities and limitations of peripheral vision. *Annu. Rev. Vis. Sci.* **2**, 437–457 (2016).
2. H. Bouma, Interaction effects in parafoveal letter recognition. *Nature* **226**, 177–178 (1970).
3. D. G. Pelli, K. A. Tillman, The uncrowded window of object recognition. *Nat. Neurosci.* **11**, 1129–1135 (2008).
4. D. Whitney, D. M. Levi, Visual crowding: A fundamental limit on conscious perception and object recognition. *Trends Cogn. Sci.* **15**, 160–168 (2011).
5. D. M. Levi, S. A. Klein, Vernier acuity, crowding and amblyopia. *Vision Res.* **25**, 979–991 (1985).
6. S. J. Crutch, E. K. Warrington, Foveal crowding in posterior cortical atrophy: A specific early visual processing deficit affecting word reading. *Cogn. Neuropsychol.* **24**, 843–866 (2007).
7. L. Parkes, J. Lund, A. Angelucci, J. A. Solomon, M. Morgan, Compulsory averaging of crowded orientation signals in human vision. *Nat. Neurosci.* **4**, 739–744 (2001).
8. J. A. Greenwood, P. J. Bex, S. C. Dakin, Crowding changes appearance. *Curr. Biol.* **20**, 496–501 (2010).
9. I. Mareschal, M. J. Morgan, J. A. Solomon, Cortical distance determines whether flankers cause crowding or the tilt illusion. *J. Vis.* **10**, 13 (2010).
10. F. Wilkinson, H. R. Wilson, D. Ellemberg, Lateral interactions in peripherally viewed texture arrays. *J. Opt. Soc. Am. A Opt. Image Sci. Vis.* **14**, 2057–2068 (1997).
11. J. A. Greenwood, P. J. Bex, S. C. Dakin, Positional averaging explains crowding with letter-like stimuli. *Proc. Natl. Acad. Sci. U.S.A.* **106**, 13130–13135 (2009).
12. R. van den Berg, J. B. T. M. Roerdink, F. W. Cornelissen, On the generality of crowding: Visual crowding in size, saturation, and hue compared to orientation. *J. Vis.* **7**, 14.1–14.11 (2007).
13. G. J. Kennedy, D. Whitaker, The chromatic selectivity of visual crowding. *J. Vis.* **10**, 15 (2010).
14. P. J. Bex, S. C. Dakin, Spatial interference among moving targets. *Vision Res.* **45**, 1385–1398 (2005).
15. A. T. Astle, D. P. McGovern, P. V. McGraw, Characterizing the role of disparity information in alleviating visual crowding. *J. Vis.* **14**, 8 (2014).
16. F. L. Kooi, A. Toet, S. P. Tripathy, D. M. Levi, The effect of similarity and duration on spatial interaction in peripheral vision. *Spat. Vis.* **8**, 255–279 (1994).
17. M. Livingstone, D. Hubel, Segregation of form, color, movement, and depth: Anatomy, physiology, and perception. *Science* **240**, 740–749 (1988).
18. L. G. Ungerleider, M. Mishkin, "Two cortical visual systems" in *Analysis of Visual Behavior*, D. J. Ingle, M. A. Goodale, R. J. W. Mansfield, Eds. (MIT Press, Cambridge, 1982), pp. 549–586.
19. S. He, P. Cavanagh, J. Intriligator, Attentional resolution and the locus of visual awareness. *Nature* **383**, 334–337 (1996).
20. H. Strasburger, Unfocused spatial attention underlies the crowding effect in indirect form vision. *J. Vis.* **5**, 1024–1037 (2005).
21. M. H. Herzog, M. Manassi, Uncorking the bottleneck of crowding: A fresh look at object recognition. *Curr. Opin. Behav. Sci.* **1**, 86–93 (2015).
22. J. A. Greenwood, P. J. Bex, S. C. Dakin, Crowding follows the binding of relative position and orientation. *J. Vis.* **12**, 18 (2012).
23. E. Põder, J. Wagemans, Crowding with conjunctions of simple features. *J. Vis.* **7**, 1–12 (2007).
24. E. H. Adelson, J. A. Movshon, Phenomenal coherence of moving visual patterns. *Nature* **300**, 523–525 (1982).
25. D. Kane, P. J. Bex, S. C. Dakin, The aperture problem in contoured stimuli. *J. Vis.* **9**, 13.1–13.17 (2009).
26. A. M. Derrington, J. Krauskopf, P. Lennie, Chromatic mechanisms in lateral geniculate nucleus of macaque. *J. Physiol.* **357**, 241–265 (1984).
27. S. G. Solomon, P. Lennie, The machinery of colour vision. *Nat. Rev. Neurosci.* **8**, 276–286 (2007).
28. C. Witzel, K. R. Gegenfurtner, Categorical sensitivity to color differences. *J. Vis.* **13**, 1 (2013).
29. X.-X. Wei, A. A. Stocker, Lawful relation between perceptual bias and discriminability. *Proc. Natl. Acad. Sci. U.S.A.* **114**, 10244–10249 (2017).
30. W. J. Harrison, P. J. Bex, A unifying model of orientation crowding in peripheral vision. *Curr. Biol.* **25**, 3213–3219 (2015).
31. C. Blakemore, R. H. S. Carpenter, M. A. Georgeson, Lateral inhibition between orientation detectors in the human visual system. *Nature* **228**, 37–39 (1970).
32. J. A. Solomon, F. M. Felisberti, M. J. Morgan, Crowding and the tilt illusion: Toward a unified account. *J. Vis.* **4**, 500–508 (2004).
33. C. Redies, L. Spillman, The neon color effect in the Ehrenstein illusion. *Perception* **10**, 667–681 (1982).
34. S. Klauke, T. Wachtler, "Tilt" in color space: Hue changes induced by chromatic surrounds. *J. Vis.* **15**, 17 (2015).
35. J. Kim, H. R. Wilson, Motion integration over space: Interaction of the center and surround motion. *Vision Res.* **37**, 991–1005 (1997).
36. A. Yashar, X. Wu, J. Chen, M. Carrasco, Crowding and binding: Not all feature-dimensions behave equally. *J. Vis.* **17**, 374 (2017).
37. R. J. Watt, M. J. Morgan, R. M. Ward, The use of different cues in vernier acuity. *Vision Res.* **23**, 991–995 (1983).
38. D. Fougnie, G. A. Alvarez, Object features fail independently in visual working memory: Evidence for a probabilistic feature-store model. *J. Vis.* **11**, 3 (2011).
39. G. A. Alvarez, P. Cavanagh, Visual short-term memory operates more efficiently on boundary features than on surface features. *Percept. Psychophys.* **70**, 346–364 (2008).
40. S. Rosen, D. G. Pelli, Crowding by a repeating pattern. *J. Vis.* **15**, 10 (2015).
41. M. Manassi, B. Sayim, M. H. Herzog, When crowding of crowding leads to uncrowding. *J. Vis.* **13**, 10 (2013).
42. B. C. Motter, D. A. Simoni, The roles of cortical image separation and size in active visual search performance. *J. Vis.* **7**, 1–15 (2007).
43. B. Balas, L. Nakano, R. Rosenholtz, A summary statistic representation in peripheral vision explains visual crowding. *J. Vis.* **9**, 13.1–13.18 (2009).
44. J. Freeman, E. P. Simoncelli, Metamers of the ventral stream. *Nat. Neurosci.* **14**, 1195–1201 (2011).
45. S. Keshvari, R. Rosenholtz, Pooling of continuous features provides a unifying account of crowding. *J. Vis.* **16**, 39 (2016).
46. R. Millin, A. C. Arman, S. T. L. Chung, B. S. Tjan, Visual crowding in V1. *Cereb. Cortex* **24**, 3107–3115 (2014).
47. M. Kwon, P. Bao, R. Millin, B. S. Tjan, Radial-tangential anisotropy of crowding in the early visual areas. *J. Neurophysiol.* **112**, 2413–2422 (2014).
48. B. C. Motter, Central V4 receptive fields are scaled by the V1 cortical magnification and correspond to a constant-sized sampling of the V1 surface. *J. Neurosci.* **29**, 5749–5757 (2009).
49. E. J. Anderson, S. C. Dakin, D. S. Schwarzkopf, G. Rees, J. A. Greenwood, The neural correlates of crowding-induced changes in appearance. *Curr. Biol.* **22**, 1199–1206 (2012).
50. M. A. Webster, Visual adaptation. *Annu. Rev. Vis. Sci.* **1**, 547–567 (2015).
51. K. Seymour, C. W. G. Clifford, N. K. Logothetis, A. Bartels, The coding of color, motion, and their conjunction in the human visual cortex. *Curr. Biol.* **19**, 177–183 (2009).
52. E. G. Louie, D. W. Bressler, D. Whitney, Holistic crowding: Selective interference between configural representations of faces in crowded scenes. *J. Vis.* **7**, 24.1–24.11 (2007).
53. M. Manassi, D. Whitney, Multi-level crowding and the paradox of object recognition in clutter. *Curr. Biol.* **28**, R127–R133 (2018).
54. A. V. Kalpadakis-Smith, V. Goffaux, J. A. Greenwood, Crowding for faces is determined by visual (not holistic) similarity: Evidence from judgments of eye position. *Sci. Rep.* **8**, 12556 (2018).
55. S. Ishihara, *Tests for Color-Blindness* (Hongo Harukicho, Tokyo, 1914).
56. D. H. Brainard, The psychophysics toolbox. *Spat. Vis.* **10**, 433–436 (1997).
57. D. G. Pelli, The VideoToolbox software for visual psychophysics: Transforming numbers into movies. *Spat. Vis.* **10**, 437–442 (1997).
58. J. A. Greenwood, M. J. Parsons, Dissociable effects of crowding for judgements of colour and motion. *J. Vis.* **16**, 234 (2016).